ADVANCED FUNCTIONAL MATERIALS
www.afm-journal.de

Inulin-Lipid Core–Shell Microcapsules Target the Gut Microbiota and Mimic the Pharmaceutical Food Effect for Improved Oral Antipsychotic Delivery

Tahlia R. Meola, Aurelia Elz, Anthony Wignall, Kara Paxton, Alexander Hunter, Amin Ariaee, Srinivas Kamath, Stephanie E. Reuter, Clive A. Prestidge, and Paul Joyce**

The oral delivery of most atypical antipsychotics is severely challenged by their low oral bioavailability and significant food effects that necessitate patient compliance. Lipid formulations are an attractive delivery system for overcoming the dosing challenges of antipsychotics, but their negative impact on the gut microbiota can interfere with the pharmacodynamic response through disruption of the gut-brain axis. Here, novel gut microbiota-targeting microcapsules are engineered to provide a multifunctional approach for improving both the pharmacokinetic and pharmacodynamic properties of the antipsychotic, lurasidone. The microcapsules are comprised of a lipid core that facilitates the solubilization and oral absorption of the lipophilic drug and an outer carbohydrate polymer (inulin) shell that positively modulates the gut microbiota by facilitating microbial fermentation. Fed-fasted variability in lurasidone solubilization is mitigated through microencapsulation with inulin-lipid microcapsules (ILM), while microbiota enrichment is coupled with enhanced serotonin levels in the small intestine, faeces, and plasma. The realization of multifunctional ILM confirms the pharmacokinetics and efficacy of mental health therapies, such as antipsychotics, can be optimized through strategic encapsulation within functional formulations that target the gut microbiota for effective modulation of the gut-brain axis.

1. Introduction

New knowledge surrounding the gut-brain axis has highlighted the importance of the gut microbiota in treating mental health conditions.[1] The microbial communities that colonise the gut regulate mood and cognition through the production of neurotransmitters and mood stabilisers (e.g., serotonin and dopamine).[2,3] Despite this, many psychotropics used for the treatment of mental health conditions negatively disrupt the gut microenvironment through antibiotic-like mechanisms and trigger a cascade of metabolic side effects, most notably, weight gain.[4,5] This is especially the case for antipsychotics used in the treatment of schizophrenia, including olanzapine, clozapine and risperidone, which induce microbiota imbalances that ultimately limit their therapeutic efficacy.[6–9]

Lurasidone, however, is an atypical antipsychotic that has been recently shown to positively modulate the gut microbiota in rats, without the commonly observed adverse effects of other atypical antipsychotics.[10] Longitudinal analyses revealed that daily lurasidone administration increased the relative abundance and diversity of the gut microbiota after just 7 days. Despite its advantageous properties toward the gut microbiota, lurasidone suffers from low aqueous solubility leading to poor oral bioavailability (in the reported range of 9–19%) and a significant pharmaceutical food effect where bioavailability varies up to 3.5-fold depending on patient food intake (or lack thereof).[11] These oral dosing challenges limit the clinical adoption of lurasidone since dosing relies on patient compliance with patients being recommended to take their medication with a meal (at least 350 kcal).[12,13] This represents a clear clinical challenge given schizophrenia and bipolar patients represent a non-compliant cohort.[14]

To overcome bioavailability challenges, lurasidone has been previously formulated with lipid-based carriers that enhance intestinal solubilization and absorption.[15–18] However, recent studies have shown that common excipients used in lipid-based formulations disrupt the gut microbiota and induce intestinal inflammation.[19–21] Given the role of the gut-brain axis in mental health, such lipid-based carriers are not feasible formulation strategies for antipsychotics. Thus, novel advanced material-based formulation strategies are urgently required for mitigating the food effect and enhancing the oral absorption of lurasidone,

T. R. Meola, A. Elz, A. Wignall, K. Paxton, A. Hunter, A. Ariaee, S. Kamath, S. E. Reuter, C. A. Prestidge, P. Joyce
UniSA Clinical & Health Sciences
University of South Australia
Adelaide, South Australia 5000, Australia
E-mail: clive.prestidge@unisa.edu.au; paul.joyce@unisa.edu.au

The ORCID identification number(s) for the author(s) of this article can be found under https://doi.org/10.1002/adfm.202403914

DOI: 10.1002/adfm.202403914

in combination with exerting positive or neutral effects on the gut microbiota.[22]

In this study, inulin-lipid core–shell microcapsules were strategically engineered to overcome antipsychotic dosing challenges by simultaneously targeting the gut microbiota and mimicking the food effect of lurasidone. Recent clinical investigations have shown that the pharmacodynamic response of antipsychotics can be enhanced by co-dosing with microbiota-active materials that positively regulate the gut-brain axis.[23–25] Therefore, inulin was selected as a microbiota-active coating for the core–shell microcapsules, given its capacity to be readily fermented by intestinal microbes, enabling widespread metabolic and mental health benefits.[26–29] It was hypothesised that the presence of inulin, a microbially accessible carbohydrate, within the formulation would mitigate dysbiosis caused by the lipid carriers, while the medium-chain triglyceride core would enable solubilization and bioavailability enhancement of the encapsulated lurasidone. Spray drying was selected as the fabrication technique due to its capacity to induce the formation of core–shell microcapsules and its common application within the pharmaceutical industry. The findings derived from this study are expected to drive the future development of microbiota-active drug delivery technologies across an array of indications, enabling these advanced materials to serve as bioactive formulations that extend the pharmacological activities of drugs, while mitigating metabolic adverse effects.

2. Results and Discussion

2.1. Spray Drying Induces the Formation of Core–Shell Inulin-Coated Lipid Microcapsules

Inulin-lipid core–shell microcapsules (ILM) encapsulating the poorly soluble antipsychotic drug, lurasidone, were fabricated by spray drying a lipid nanoemulsion (227 ± 31 nm) dispersed within an inulin solution (**Figure 1A**). The dehydration process induced the formation of smooth, spherical microcapsules (Figure 1B), 6.51 ± 2.60 µm in mean diameter, with a core–shell structure where a lipid core was encapsulated within an inulin shell, evidenced through cross-sectional scanning electron and confocal fluorescent micrographs (Figure 1C,D). The lipid loading within the spray-dried microcapsules was 40.6 ± 2.2%, representing a lipid encapsulation efficiency of >80%. Lurasidone was encapsulated within the microcapsules at a total drug loading of 0.65 ± 0.1% (93% encapsulation efficiency).

While the drug loading was low in this formulation, it is important to highlight that maximizing drug loading was not a priority in this study given lurasidone necessitates a relatively low clinical dose (typical starting dose of 20 mg per day) and sufficient inulin content was necessary within the formulation for microbiota modulation. Previous studies have highlighted that inulin at doses of 2 g kg^{-1} and 12 g day^{-1} in rodent preclinical [30] and human clinical models,[31] respectively, can positively modulate the gut-brain axis during schizophrenia treatment. Doses of 20 mg k^{-1} g for the single dose pharmacokinetic study and 7.5 mg k^{-1} g for the daily dose pharmacodynamic study represent relative inulin doses of ≈1.8 g kg^{-1} and 700 mg k^{-1} g, respectively. Thus, it was hypothesized that the inulin doses within the formulation would be sufficient to induce microbiota modulation, while effectively delivering lurasidone.

2.2. Inulin-Lipid Core–Shell Microcapsules Mitigate the Pharmaceutical Food Effect by Promoting Lurasidone Solubilization

The capacity for ILM to increase the solubilization and overcome the food effect of lurasidone was investigated during in vitro lipolysis under biorelevant conditions simulating gastrointestinal digestion in both the fasted and fed state. In the fasted state, lurasidone was rapidly solubilized within the gastric phase with 65.6 ± 12.3% of the pure drug solubilized after 1 min (**Figure 2A**). However, upon phase transitioning to simulated intestinal media (after 30 min of gastric lipolysis), lurasidone solubility immediately decreased, resulting in a final solubilization of <20%. The pH-dependent solubilization profile observed for lurasidone is characteristic of poorly soluble weak bases due to their propensity to precipitate when converting from an ionized form in the low pH gastric phase to their insoluble, non-ionized form in the more neutral pH intestinal phase.[32,33] A similar pH-dependent solubilization profile was observed for the lipid nanoemulsion, however, a 2.5-fold increase in the extent of intestinal solubilization was observed, highlighting the capacity for the lipid and its digestion products to solubilize lurasidone.[16] In vitro lipolysis data indicated that over 60% of the lipid nanoemulsion was digested within the 60 min intestinal lipolysis period (Figure 2B), confirming a mix of fatty acids, monoglycerides, diglycerides and undigested triglycerides were present in the lipolysis media.

Encapsulating lurasidone within inulin microparticles delayed the rapid drug release within the gastric phase, in line with previous studies that demonstrated sustained drug release behaviour from spray-dried inulin microparticles, mediated by the erosion of the inulin matrix.[34] While inulin microparticles provided a little overall benefit to intestinal solubilization, the slightly increased extent of solubilization demonstrates that inulin does provide a slight hydrophobic microenvironment that prevented the complete intestinal precipitation of lurasidone. This is especially highlighted for ILM, where equivalent delayed release kinetics during the gastric phase were observed, followed by a significant increase in intestinal solubilization compared to the other formulations (Figure 2A). The increase in fasted-state intestinal solubilization of lurasidone in ILM demonstrates a synergistic effect facilitated by the hybrid microcapsules, where the lipid in combination with inulin promotes the solubilization of lurasidone while inhibiting drug recrystallization. Lipolysis kinetics of ILM were sustained compared to the lipid nanoemulsion, suggesting lipase bioaccessibility to the lipid interface is restricted, likely due to the presence of the inulin shell and the reduced interfacial surface area in contrast to the lipid nanoemulsion.[32]

Solubilization of lurasidone was significantly lower in the gastric phase under simulated fed state conditions for all formulations (Figure 2C). This is due to lurasidone being a weak base with a pKa of 7.6 and a pH-dependent solubility. Intestinal solubilization was significantly enhanced for the pure drug due to the increased concentration of solubilizing lipids and bile salts within the media, providing clear evidence for the characteristic food effect of lurasidone. Drug solubilization was also significantly increased for the lipid nanoemulsion, reaching a maximum solubilization of 86.9 ± 2.7% after 5 min of the intestinal phase, prior to declining over the remainder of the lipolysis

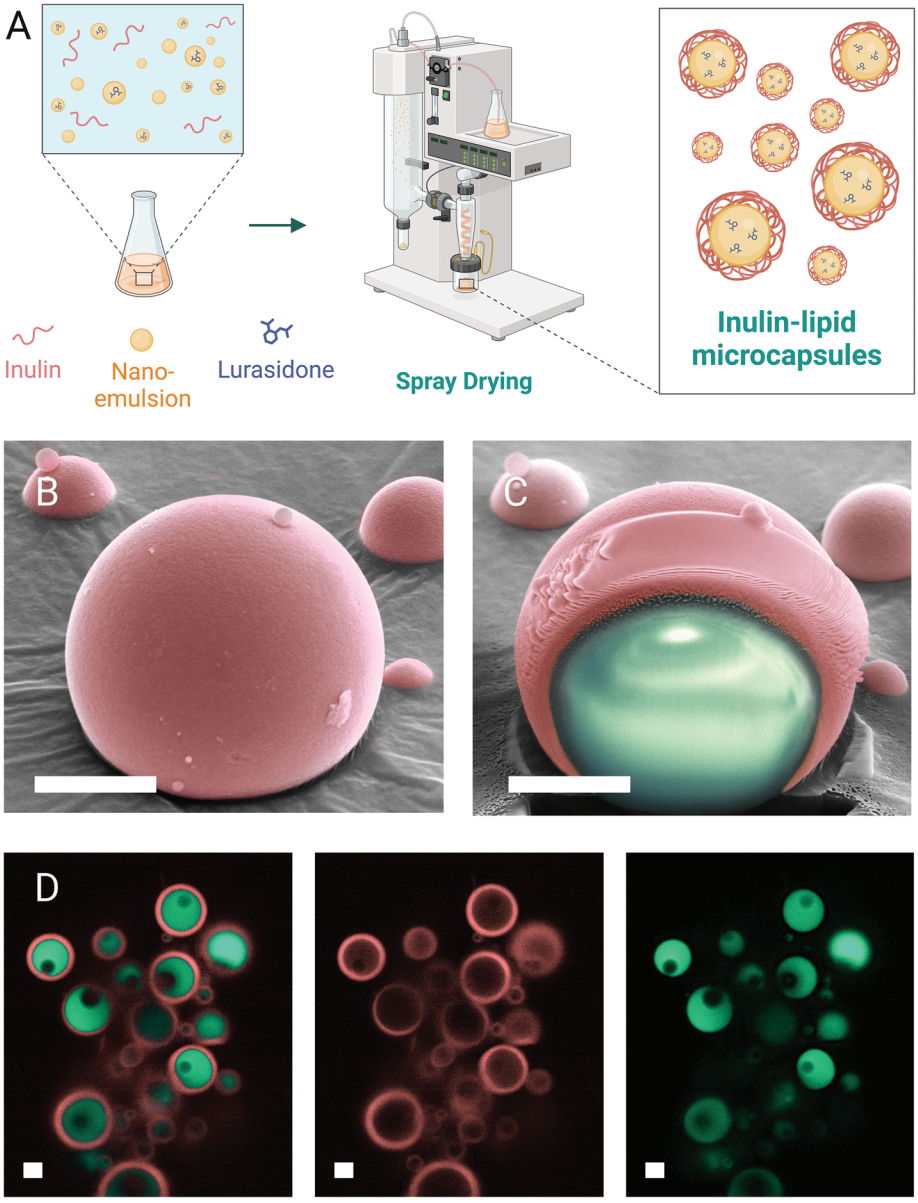

Figure 1. Inulin-lipid core–shell microcapsules were fabricated by spray drying a lipid nanoemulsion with inulin dispersed within the aqueous phase at a 1:1 lipid: inulin ratio. A) Schematic representation of the synthesis process, where lurasidone was solubilized within medium-chain triglycerides which were dispersed in an inulin solution to form a nanoemulsion. The subsequent nanoemulsion was spray-dried to form ILM. B. Scanning electron micrographs revealed smooth, spherical microcapsules, with cross-sectional analysis via FIB-SEM revealing a core–shell structure (Panel C), confirmed with confocal fluorescence micrographs (Panel D) where it was evident that a lipid core (green) was encapsulated within an inulin shell (pink). Scale bars = 5 μm.

period due to drug precipitation. Importantly, the degree of drug solubilization for inulin microparticles and ILM did not differ significantly between the simulated fasted and fed states, resulting in fed: fasted solubilization ratios ≈1 (Figure 2E), which significantly contrasts the fed: fasted solubilization ratios of 2.65 ± 0.4 and 1.76 ± 0.2 for the pure drug and lipid nanoemulsion, respectively. Importantly, this highlights the capacity for the inulin-based hybrid formulations to mitigate the pharmaceutical food effect of lurasidone, which is a major dosing challenge and patient compliance issue for the drug.

2.3. Inulin-Lipid Core–Shell Microcapsules Enhance Oral Lurasidone Bioavailability

The pharmacokinetic profiles for each formulation following a single oral dose of lurasidone (20 mg k^{-1} g) to male Sprague–Dawley rats are presented in **Figure** 3A with corresponding pharmacokinetic parameters detailed in **Table** 1. No significant difference was observed between the pharmacokinetic profiles of the pure drug and inulin microparticles, with area-under-the-curve ($AUC_{0\text{-}24}$) values of 123 ± 36 ng h mL^{-1} and 189 ± 36 ng h mL^{-1} (Figure 3B), respectively. This indicates

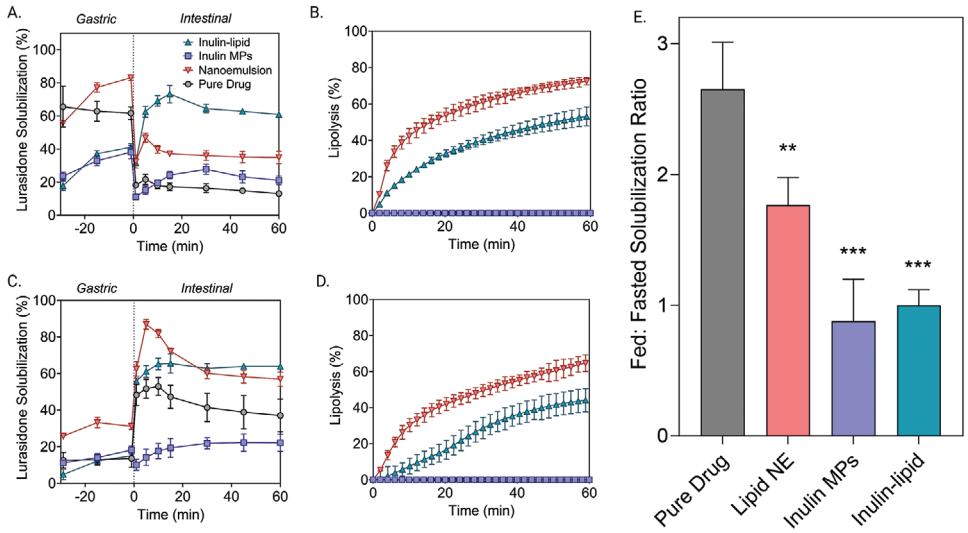

Figure 2. Inulin-lipid microcapsules (ILM) enhance lurasidone solubilization and mitigate the pharmaceutical food effect in vitro. In vitro lurasidone solubilization and lipid hydrolysis under simulated fasted A,B, respectively) and fed C,D, respectively) state conditions. E) Fed: fasted state solubilization ratios for the various formulation groups highlight equivalent lurasidone solubilization capacity for ILH under fed and fasted state conditions. Values represent the mean ± SD, $n = 4$. Statistical significance was determined using an unpaired *t*-test and one-way ANOVA followed by Tukey's post-test for multiple comparisons ($^{*}p < 0.05$, $^{**}p < 0.005$, $^{***}p < 0.0005$ or $^{****}p < 0.0005$).

that encapsulating lurasidone within an inulin matrix, in the absence of a lipid core, does not facilitate improved drug absorption. In contrast, the lipid nanoemulsion facilitated a 2.5-fold increase in oral bioavailability, evidenced by an $AUC_{0\text{-}24}$ value of 303 ± 42 ng h mL^{-1}, along with a more sustained absorption profile with a T_{max} of 4.00 ± 2.0 h and a half-life of 5.15 ± 0.5 h. Importantly, ILM drastically increased the oral bioavailability of lurasidone by 8.8- and 3.6-fold compared to the pure drug and lipid nanoemulsion, respectively (Figure 3A,B).

In vitro-in vivo correlations (IVIVC) existed between in vitro solubilization data and pharmacokinetic parameters (Figure 3C,D), indicating that the enhanced pharmacokinetic performance of ILM is likely attributed to the capacity for ILM to facilitate solubilization of lurasidone within the gastrointestinal tract. To fully establish these correlations, it is necessary to investigate additional formulations to provide sufficient data points for conclusively assessing IVIVC. The order of magnitude improvement in oral bioavailability facilitated by ILM further confirms a synergistic mechanism of action is present for the microcapsules, whereby it is demonstrated the lipid component facilitates the solubilization of the poorly soluble drug, while the inulin shell both limits the rate of drug release and prevents drug precipitation in the intestinal tract. Previous studies have demonstrated the capacity for carbohydrate polymers (e.g., cellulose derivatives and natural gums) to serve as polymeric precipitation inhibitors (PPIs) by restricting the recrystallization of poorly soluble drug compounds in the GI tract (see detailed review),[35] which has led to PPIs being frequently combined with lipid-based formulations for a synergistic effect.[36–38] Thus, it is anticipated that inulin provides a similar precipitation inhibitory effect as previously explored carbohydrate polymers, but additional mechanistic and characterization studies that demonstrate the capacity for inulin to prevent crystal nucleation are necessary.

2.4. Lurasidone Formulations Alter Gut Microbiota Composition and Diversity in a Formulation-Dependent Manner

Lurasidone formulations were orally administered to Sprague–Dawley rats ($n = 8$; four male and four female per group) at a lurasidone dose of (7.5 mg k^{-1} g) for 21 days to investigate their impact on the gut microbiota, intestinal health, and serotonin levels in the small intestine, faeces, and plasma. The dose, frequency of administration, and length of study were selected to simulate a chronic dosage regimen, given most schizophrenia and bipolar disorder patients are prescribed antipsychotic medication (including lurasidone) over an extended treatment course. 16S sequencing of faecal samples collected on Day 21 revealed distinct microbial signatures for animals receiving the various treatment groups, with the relative abundance of microbes (at the family taxonomic level) for each animal presented in **Figure** 4A and grouped relative abundance data presented in Figure 4B. Evidence of microbiota enrichment by the pure drug, inulin microparticles and ILM, compared to the control group and lipid nanoemulsion, was observed through statistically significant increases in operational taxonomic units (OTUs; Figure 4C) and alpha diversity (Shannon's Index, Figure 4D). Principal component analysis (PCoA) revealed a statistically significant shift ($p < 0.05$) in gut microbiota composition for all groups administered with lurasidone formulations in contrast to the control group (i.e., PBS only), highlighted by the separation between PCo1 and PCo2 in Figure 1E. However, PERMANOVA (Bray-Curtis) of multidimensional beta diversity revealed that only the group administered the lipid nanoemulsion triggered statistically significant ($p < 0.05$) microbiota composition shifts compared to the pure drug.

To further elucidate the impact of the lurasidone-loaded lipid nanoemulsion on the gut microbiota, longitudinal analyses were

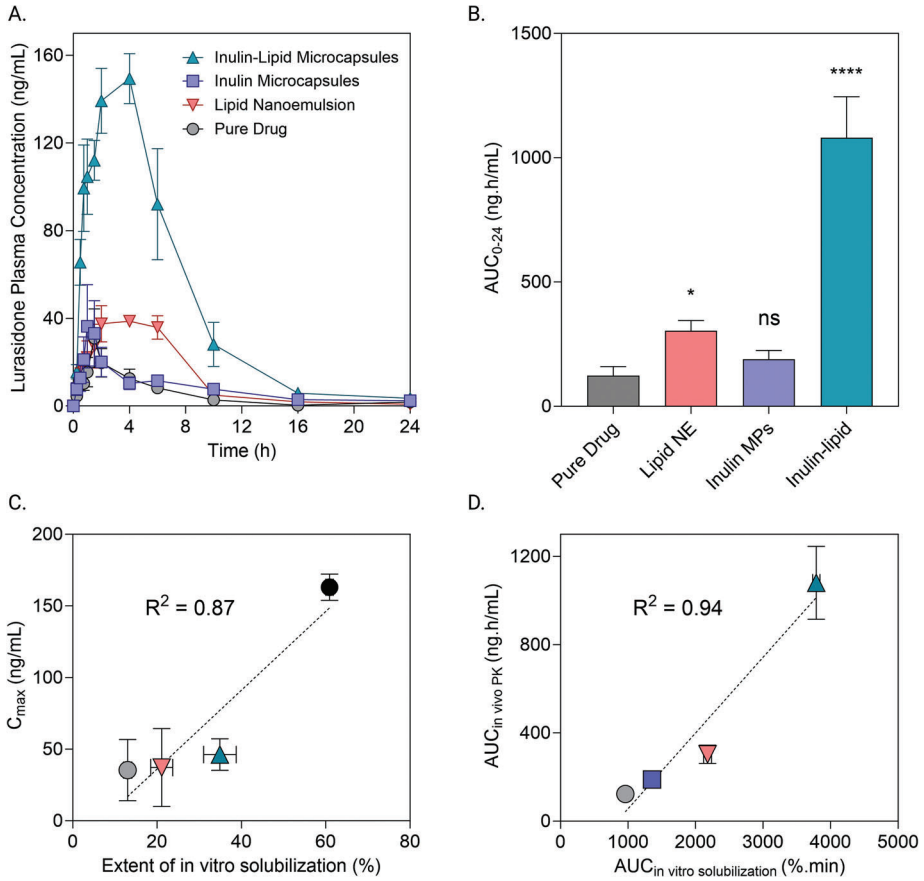

Figure 3. Oral lurasidone bioavailability is enhanced 8.7-fold when formulated with inulin-lipid hybrid microparticles. A) In vivo pharmacokinetic profiles demonstrate improved lurasidone absorption following oral administration to Sprague-Dawley rats in the fasted state, corresponding with a significantly greater area under the curve (Panel B). In vitro-in vivo correlations (IVIVC) indicate that the extent of in vitro lurasidone solubilization correlates with C_{max} (Panel C) and AUC of in vitro intestinal solubilization profiles correlates with AUC of in vivo pharmacokinetic profiles (Panel D), in the fasted state. Values represent the mean ± SD, $n = 4$. Statistical significance was determined using an unpaired *t*-test and one-way ANOVA followed by Tukey's post-test for multiple comparisons ($^{*}p < 0.05$, $^{**}p < 0.005$, $^{***}p < 0.0005$ or $^{****}p < 0.0005$).

performed by contrasting microbial signatures from individual animals on Day 0 (i.e., before the first dose) and Day 21 (i.e., after the final dose). Differential abundance analyses revealed that key commensal taxa at the family taxonomical level were depleted following 21 days of lipid nanoemulsion dosing (**Figure 5A**), demonstrating the capacity for the lipid nanoemulsion to trigger a dysbiotic state through the depleted abundance of commensal microbial populations. The dysbiotic state was further characterized by longitudinal reductions in OTUs (Figure 5B) and Shannon's index (Figure 5C). PERMANOVA (Bray-Curtis) of multidimensional beta diversity revealed statistically significant differences ($p = 0.0008$) in the composition of the microbiota between Day 0 and Day 21, as clearly evidenced through the separation of PCo1 (Figure 5D).

These findings are in agreement with a recent study that showed the capacity for lipid-based drug delivery formulations to trigger gut microbiota dysbiosis in rats.[19] It was highlighted that formulations comprising a lipid and surfactant phase depleted the abundance and diversity of the microbiota, corresponding with an increased pro-inflammatory response in the small intestine. However, in the previous study, no drug was present and only the lipid formulation being dosed. Thus, this study is the

Table 1. Pharmacokinetic parameters following oral administration of lurasidone (20 mg k^{-1} g) formulations to Sprague Dawley rats in the fasted state. Values represent the mean ± SD, $n = 4$.

Pharmacokinetic parameter	Pure lurasidone	Nanoemulsion	Inulin microcapsules	Inulin-lipid microcapsules
T_{max} (h)	1.38 ± 0.629	4.00 ± 2.00	1.17 ± 0.289	3.33 ± 1.15
C_{max} (ng mL^{-1})	35.4 ± 21.4	46.3 ± 11.0	37.2 ± 27.2	163 ± 9.24
AUC_{0-24} (ng h mL^{-1})	123 ± 36.2	303 ± 41.8	189 ± 35.8	1080 ± 165
AUC_{inf} (ng h mL^{-1})	130 ± 42.6	308 ± 43.1	196 ± 13.2	1200 ± 28.4
$T_{1/2}$ (h)	1.98 ± 0.525	5.15 ± 0.545	7.92 ± 0.458	3.98 ± 0.116

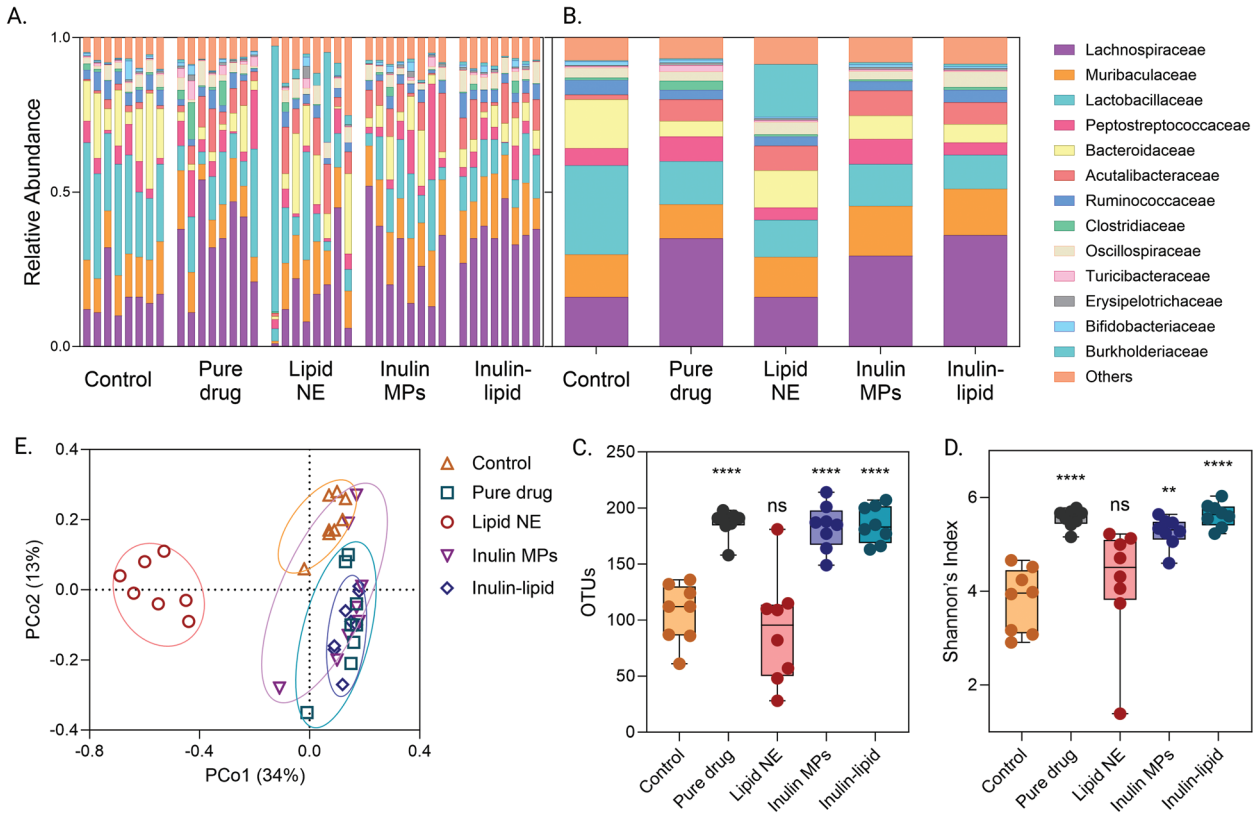

Figure 4. Lurasidone formulations trigger formulation-dependent changes in the gut microbiota. A) The relative abundance of gut microbes at the family taxonomical level for individual animals within each treatment group ($n = 8$). B) Grouped mean relative abundances for each treatment group at the family taxonomical level. Changes in OTUs (Panel C) and alpha diversity (characterized by Shannon's index) (Panel D) revealed the pure drug, inulin microparticles and inulin-lipid microcapsules enriched the gut microbiota. Principal component analyses (Panel E) show statistically significant shifts in microbiota compositions for all lurasidone formulation groups relative to the control. Statistical significance was determined using an unpaired *t*-test and one-way ANOVA followed by Tukey's post-test for multiple comparisons ($^{*}p < 0.05$, $^{**}p < 0.005$, $^{***}p < 0.0005$ or $^{****}p < 0.0005$).

first to demonstrate that lipid formulations still significantly disrupt gut flora while encapsulating a drug with a proven capacity to positively modulate microbiota composition. Ultimately, this highlights that caution must be taken when utilizing liquid lipid-based formulations for the bioavailability enhancement of poorly soluble drugs, given their capacity to detrimentally modulate the gastrointestinal microenvironment. While demonstration of this relationship in clinical studies is necessary, these findings represent an opportunity for the development of new microbiota-targeting drug delivery vehicles that positively modulate the gut microbiota while also enhancing the oral bioavailability of encapsulated drugs.[22]

2.5. Inulin-Lipid Core–Shell Microcapsules Promote a Diverse Gut Microbiota and Attenuate Intestinal Inflammation Induced by the Liquid Lipid Nanoemulsion

Intergroup comparisons of multi-dimensional beta diversity at Day 21 (Figure 4E) using PERMANOVA (Bray–Curtis) revealed statistically significant ($p = 0.0001$) microbiota shifts between the lipid nanoemulsion and ILM, suggesting the impact of both formulations on the gut microbiota varied considerably. To elucidate this further, longitudinal analyses were performed by contrasting microbial signatures from individual animals receiving ILM on Day 0 (i.e., before the first dose) and Day 21 (i.e., after the final dose). In contrast to the lipid nanoemulsion, the enrichment of key commensal taxa at the family taxonomical level was observed following ILM dosing (**Figure 6**A), corresponding with significant increases in OTUs (Figure 6B) and Shannon's Index (Figure 6C), demonstrating that the formulation facilitated the expansion and increased diversity of the microbiota. PERMANOVA (Bray–Curtis) of multi-dimensional beta diversity revealed statistically significant differences ($p = 0.0002$) in the composition of the microbiota between Day 0 and Day 21, as clearly evidenced through the separation of PCo1 (Figure 6D). This highlights that the inulin shell of ILM enables the expansion of microbial communities within the GI tract by providing a source of fermentable energy to bacteria, ultimately leading to an increase in microbial abundance (i.e., OTUs) and diversity (i.e., Shannon's index). This is despite the presence of a lipid nanoemulsion core within ILM, suggesting that the presence of inulin at a 1:1 ratio within this formulation is sufficient for protecting against negative formulation-induced microbiota effects.

Intestinal inflammation caused by the various treatments was investigated at study completion by quantifying the relative levels of pro-inflammatory cytokines (IL-1β, IL-6, and

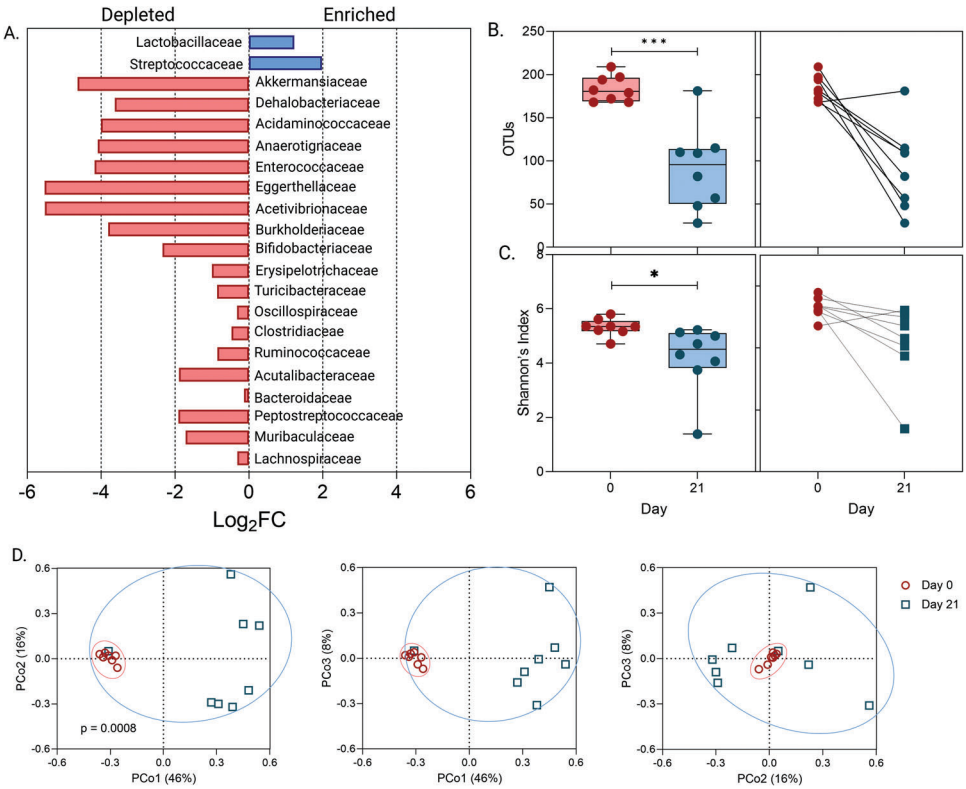

Figure 5. The lipid nanoemulsion induces gut dysbiosis through longitudinal shifts in gut microbiota composition, abundance and diversity. A) Log_2 fold changes (Log_2FC) highlighting differentially abundant taxa in the gut microbiota between Day 0 and Day 21, where a negative Log_2FC represents depleted abundance (red) and a positive Log_2FC represents enriched abundance (blue). Changes in OTUs (Panel B) and alpha diversity (characterized by Shannon's index) (Panel C) revealed the lipid nanoemulsion depleted the gut microbiota. Principal component analyses (Panel D) show statistically significant shifts in microbiota compositions between Day 0 and Day 21 following treatment with the lurasidone-loaded lipid nanoemulsion dosed daily at 7.5 mg k^{-1} g of lurasidone ($n = 8$). Statistical significance was determined using an unpaired *t*-test and one-way ANOVA followed by Tukey's post-test for multiple comparisons ($^{*}p < 0.05$, $^{**}p < 0.005$, $^{***}p < 0.0005$ or $^{****}p < 0.0005$).

TNF-α) within jejunal tissue. Consistent with previous findings, the pure drug did not trigger an increase in the pro-inflammatory response compared to the control group (Figure 6E–G).[10] In contrast, the lipid nanoemulsion triggered statistically significant increases in each cytokine, suggesting that formulation-induced changes to the gut microbiota are associated with a pro-inflammatory response.[19] ILM mitigated this inflammatory response through overall reductions in pro-inflammatory cytokine expression compared to the control group ($p > 0.05$), pure drug ($p > 0.05$), and lipid nanoemulsion ($p < 0.05$). Previously, the pro-inflammatory response triggered by lipid-based formulations was shown to directly correlate with changes to microbiota abundance (i.e., OTUs) and diversity (i.e., Shannon's index).[19] Thus, the capacity for ILM to mitigate a pro-inflammatory response through increased cytokine expression can be attributed to the positive enrichment of microbiota abundance and diversity enabled by the inulin shell, despite the presence of a lipid nanoemulsion core within ILM. Importantly, this formulation engineering approach, therefore, enables the use of lipid-based formulations for bioavailability enhancement without compromising intestinal health through detrimental changes to the gut microbiota.

2.6. Inulin-Coated Lipid Microcapsules Enhance Systemic and Faecal Serotonin Levels

Due to the complex pathogenesis of schizophrenia and bipolar disorder, antipsychotics exert multi-targeted modes of action to regulate neurotransmitter signalling via interactions with serotonergic, muscarinic, adrenergic, and histaminergic receptors.[39] Lurasidone is a serotonin (5-HT) and dopamine antagonist.[13] Given over 95% of serotonin biosynthesis occurs in the gastrointestinal tract,[40] for which the microbiota plays an integral and multifaceted role in serotonin expression, signalling, and synthesis,[41] the impact of lurasidone formulation on systemic and intestinal serotonin levels was investigated. The pure drug triggered a statistically significant increase in serotonin concentration within both plasma and faecal samples (**Figure** 7A,B), which can largely be expected due to lurasidone's antagonistic effect on 5-HT2A receptors.[14] Serotonin levels were equivalent to the control group when lurasidone was administered with the lipid nanoemulsion, while inulin microparticles induced an equivalent increase in serotonin levels to the pure drug. In contrast, ILM induced a 20-fold and 2.2-fold increase in systemic serotonin concentrations, compared to the control group and pure drug, respectively. This coincided with a 3.9-fold and

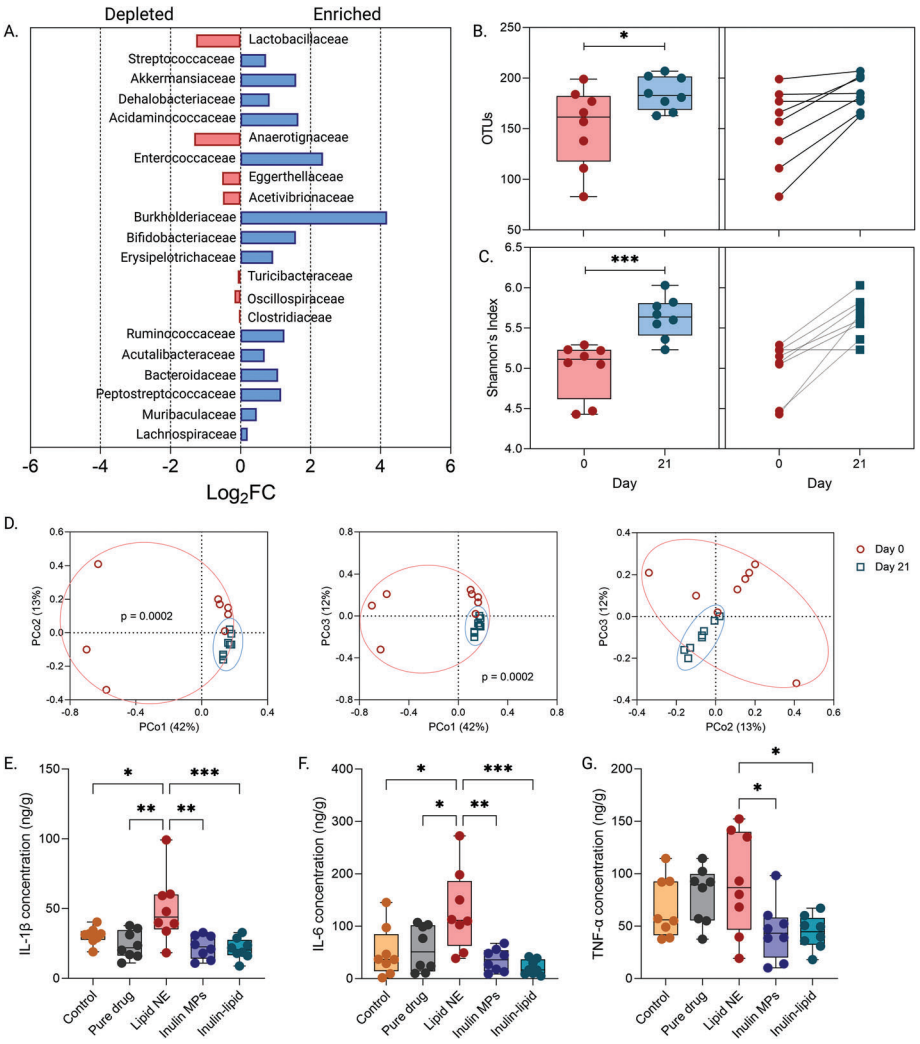

Figure 6. Inulin-lipid microcapsules boost gut microbiota abundance and diversity while reducing intestinal inflammation in contrast to a lipid nanoemulsion. A. Log_2FC for differentially abundant taxa in the gut microbiota between Day 0 and Day 21, with inulin-lipid microcapsules enriching the abundance of several commensal taxa (blue) while depleting few commensal taxa (red). Changes in OTUs (Panel B) and alpha diversity (characterized by Shannon's index) (Panel C) further revealed the capacity for inulin-lipid microcapsules to enrich the gut microbiota. Principal component analyses (Panel D) showed statistically significant shifts in microbiota compositions between Day 0 and Day 21 following daily treatment with the inulin-lipid microcapsules dosed at 7.5 mg k^{-1} g of lurasidone. Quantification of pro-inflammatory cytokine levels, specifically IL-1β (Panel E), IL-6 (Panel F), and TNF-α (Panel G), within jejunal tissue revealed the capacity for inulin-lipid microcapsules to mitigate intestinal inflammation when compared to the lipid nanoemulsion. Values represent the mean ± SD, $n = 8$. Statistical significance was determined using an unpaired *t*-test and one-way ANOVA followed by Tukey's post-test for multiple comparisons ($^{*}p < 0.05$, $^{**}p < 0.005$, $^{***}p < 0.0005$ or $^{****}p < 0.0005$).

1–6-fold increase in faecal serotonin levels compared to the control group and pure drug, respectively.

The enhanced systemic and faecal serotonin concentrations observed following ILM administration are likely due to its multifaceted mechanism of action. That is the 8.8-fold increase in lurasidone bioavailability mediated by ILM results in more drugss systemically available to exert its pharmacological mechanism, while the increase in abundance and diversity of gut microbes in the presence of ILM is expected to lead to greater serotonin biosynthesis and signalling.[42] Weak correlations existed between pharmacokinetic parameters and systemic serotonin levels (Figure 7C,D), but due to the lack of data points it is challenging to draw strong conclusions. It must also be noted that the serotonin levels were measured in animals receiving multiple doses, while the pharmacokinetic parameters were measured in animals receiving a single lurasidone dose. In contrast, microbiota diversity and abundance correlated through casual trends with plasma and faecal serotonin levels (Figure 7E–H), suggesting that ILMs gut microbiota-modulating capacity may serve as a mechanism for enhancing the pharmacodynamic response to lurasidone. These findings provide the platform for future work that focuses on understanding the impact of ILM on anti-psychotic treatment efficacy in schizophrenia disease models, where focus should be attributed to understanding the holistic impact of ILM on neurotransmitter synthesis and signalling, beyond serotonin. Further, future work should focus on

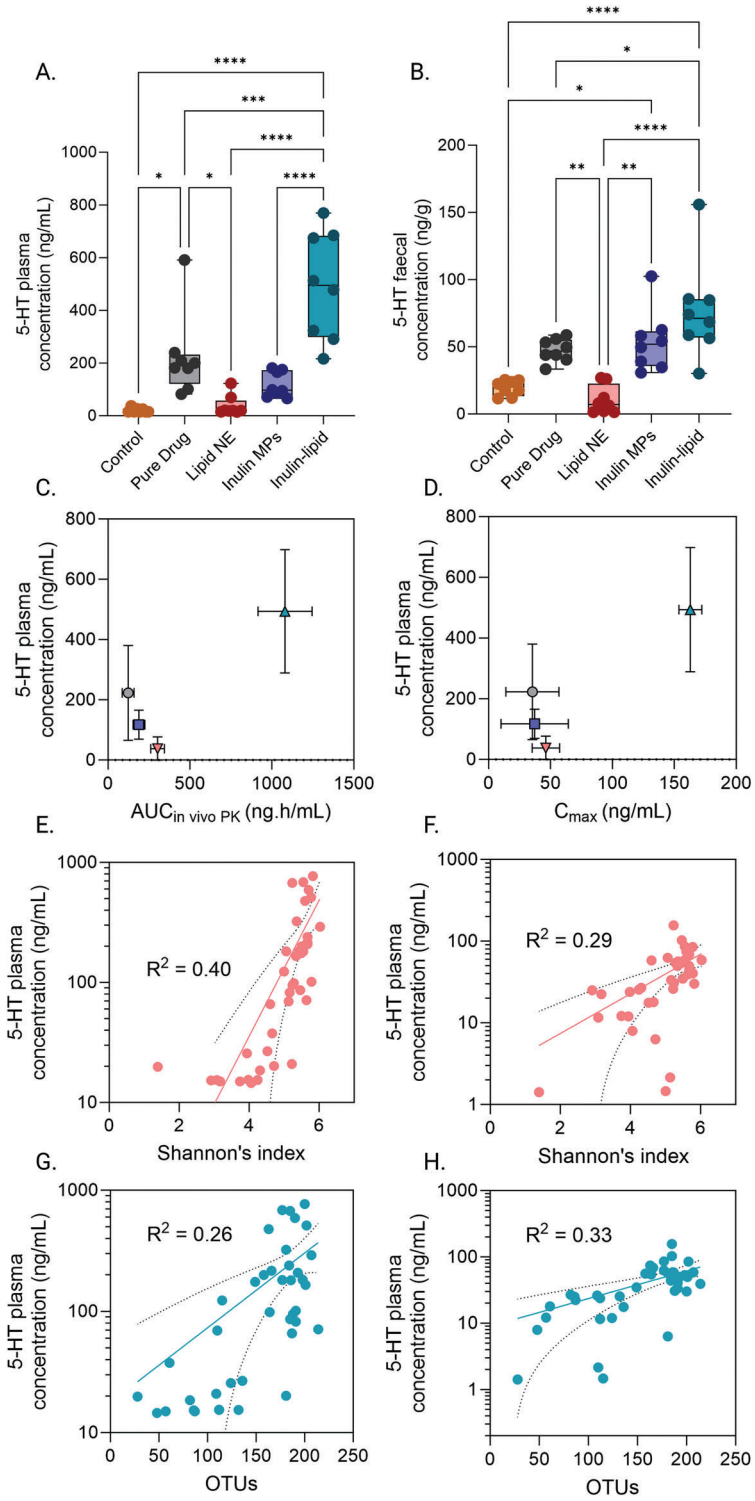

Figure 7. Inulin-lipid microcapsules facilitate an increase in systemic and faecal serotonin concentrations, correlating with an increased abundance and diversity of the gut microbiota. Serotonin (5-HT) concentrations were observed in plasma (Panel A) and faecal samples (Panel B) for the various lurasidone formulations. Panel C and D demonstrate that serotonin levels in plasma poorly correlate with pharmacokinetic parameters, being AUC and C_{max}, respectively. Correlations suggest trends exist between microbiota diversity (Shannon's Index) and plasma and faecal serotonin concentrations (Panel E,F), and microbiota abundance (OTUs) plasma and faecal serotonin concentrations (Panel G-H). Values represent the mean ± SD, $n = 8$. Statistical significance was determined using an unpaired *t*-test and one-way ANOVA followed by Tukey's post-test for multiple comparisons ($^{*}p < 0.05$, $^{**}p < 0.005$, $^{***}p < 0.0005$ or $^{****}p < 0.0005$).

understanding the impact of key ILM properties, such as particle size and composition, on bioavailability enhancement and gut microbiota enrichment to provide an avenue for optimising antipsychotic treatment efficacy.

3. Conclusion

The current study is the first of its kind to demonstrate that advanced oral drug formulations can be strategically engineered to increase the pharmacokinetic and pharmacodynamic properties of antipsychotic drugs. By engineering lipid microcapsules with an inulin coating, the pharmaceutical food effect of lurasidone was mitigated through >8-fold improved oral absorption while increasing the abundance and diversity of the gut microbiota. The microbiota-targeting effects of the inulin-lipid microcapsules demonstrated initial proof-of-concept for altering the pharmacodynamic performance of lurasidone through enhanced systemic and faecal serotonin levels, weakly correlating with pharmacokinetic and microbiota profiles. Ultimately, this study presents new opportunities for enhancing antipsychotic therapies, while also demonstrating the capacity to engineer functional oral drug formulations that go beyond pharmacokinetic enhancements.

4. Experimental Section

Materials: Lurasidone and ziprasidone powders with purity >99.0% were purchased from Hangzhou Dayangchem Co. Ltd. (Hangzhou City, China). Inulin from dahlia tubers (with a degree of polymerization of 35), soybean lecithin, phosphate-buffered saline (PBS), 4-bromophenylboronic acid (4-BBA), 1,2- dioleoyl-3-[16-N-(lissamine rhodamine B sulfonyl) amino]palmitoyl-sn-glycerol, FITC-inulin, and deuterium oxide (D_2O) were purchased from Merck (Bayswater, Australia). Capmul MCM, a mix of medium-chain glycerides, was kindly supplied by Abitec Pty Ltd (NSW, Australia). 3F (FaSSIF/FeSSIF/FaSSGF) powder was purchased from Biorelevant.com Ltd (London, United Kingdom). Porcine pancreatin extract (activity equivalent to 8 × USP specification) was supplied by MP Biomedicals (Seven Hills, Australia). Heparin sodium and saline 0.9% were purchased from Lyppard Australia (Beverley, Australia). All chemicals and solvents were of analytical grade and used as received. High-purity Milli-Q water was used throughout the study.

Fabrication and Characterization of Lurasidone Delivery Systems—Nanoemulsion Synthesis: Lurasidone (1.4% w/w) was dissolved in a lipid phase comprising of Capmul MCM (5 g) and lecithin (6% w/w) with the aid of sonication (30 min), prior to the addition of water (100 mL) to form a 5% w/v lipid-in-water emulsion. The resulting emulsion was sonicated for 1 h to facilitate size reduction and the production of a nanoemulsion.

Fabrication and Characterization of Lurasidone Delivery Systems—Inulin-Lipid Microcapsules (ILM) Synthesis: ILM was synthesized by using a spray drying approach reported previously,[34] where the lurasidone nanoemulsion was combined with an inulin solution (2% w/v) at a 1:1 lipid: inulin ratio. The nanoemulsion containing inulin in the aqueous phase and lurasidone solubilized in the lipid phase was spray-dried using a Mini Spray Dryer B-290 (Büchi Labortechnik AG) under the following conditions: emulsion flow rate: 0.5 mL $mi^{-1}n$, air flow rate: 0.6 mL min^{-1}, inlet temperature: 200 °C, outlet temperature: 110 °C, and an aspirator setting of 100%.

To contrast the performance of ILM, inulin microcapsules (IM) without a lipid phase were synthesised by dissolving lurasidone at its maximum solubility (i.e., 0.2 mg mL^{-1}) within the aqueous phase of the 2% w/v inulin solution, prior to spray drying. Spray drying conditions were equivalent to that of ILM.

Quantification of Drug Loading via Liquid Chromatography-Mass Spectrometry (LCMS): To determine lurasidone loading within ILH, ≈10 mg of powder was dissolved in acetonitrile (10 mL) and sonicated for 30 min. Aliquots (1 mL) were centrifuged for 15 min at 8944 g and the supernatants were collected and diluted for liquid chromatography-mass spectrometry (LCMS) analysis. LCMS was used for the analysis of unknown lurasidone concentrations throughout the entirety of the study (i.e., drug loading, in vitro solubilization, and in vivo pharmacokinetics analysis), with ziprasidone serving as the internal standard. A gradient elution protocol was adopted on a Shimadzu LCMS 8030 system (Kyoto, Japan) equipped with a Kinetex C18 100A column (50 × 3 mm × 1.7 µm). Specific details of the protocol employed have been previously reported.[16] Ion detection was performed in multiple reaction monitoring mode using positive electrospray ionisation, with mass-to-charge rations (m/z) of 413.2/194 and 493.2/166.1 for lurasidone and ziprasidone, respectively. The limit of detection (LOD) and limit of quantification (LOQ) for lurasidone was 0.3 ng mL^{-1} and 0.5 ng mL^{-1}, respectively.

Physicochemical Characterization: The particle size of the nanoemulsion and ILM was evaluated by using dynamic light scattering (Zetasizer Nano ZS, Malvern Instruments, Worcestershire, UK) and laser diffraction (Malvern Mastersizer, Malvern Instruments), respectively, using a refractive index of 0.145. All measurements were performed in triplicate.

Focused Ion Beam Scanning electron microscopy (FIB-SEM; FEI Helios Nanolab 600, Thermo Scientific) was used to observe the morphology and cross-sectional structure of ILM, by placing a powder sample on carbon tape and sputter-coating with a thin layer of carbon prior to imaging. A layer of platinum (Pt) was deposited to protect the sample surface toward selective milling of a site-specific area for cross-sectional analysis. Milling was performed under vacuum by using a high energy gallium ion beam to mill the target area precisely and real-time monitoring in both electron and ion beams. A high current (9.3 nA at 30 KV) was used for rough milling followed by gentle polishing with subsequent low currents (6.5 nA, 2.8 nA, 0.92 nA, 0.28 nA and 93 pA at 30 KV). Ultra hi-resolution SEM images were acquired with the help of in-lens detector.

Confocal fluorescence imaging analysis (Zeiss LSM800, Oberkochen, Germany) was performed using fluorescently labelled ILM that was prepared by adding (prior to spray drying) 0.1 wt% rhodamine-labelled triglyceride, 1,2- dioleoyl-3-[16-N-(lissamine rhodamine B sulfonyl) amino]palmitoyl-sn-glycerol, and 0.1 wt% FITC-inulin to the lipid and inulin phase, respectively. Confocal micrographs were detected at the emission wavelength of 580 nm for rhodamine (excitation wavelength 556 nm) and 519 nm for FITC (excitation wavelength 495 nm), which are represented as green and pink, respectively.

Proton nuclear magnetic resonance (^{1}H NMR) spectroscopy was used to characterize the relative lipid content within ILM by comparing the relative wavelength intensities of peaks between 1.1 and 1.4 ppm (correlating to lipid protons) and 4.3–4.8 ppm (correlating to inulin protons). To determine unknown lipid concentrations, a standard curve of relative wavelength intensities was established for varying inulin: lipid ratios between 5: 95 and 95: 5.

In Vitro Drug Solubilization Studies—Preparation of Biorelevant Gastrointestinal Media: A two-step gastrointestinal (GI) in vitro lipolysis model adapted from[33] was employed to test the solubilization of lurasidone under digesting conditions. 3F (FaSSIF/FeSSIF/FaSSGF) powder was used to prepare fasted-state gastric (FaSSGF; pH 1.6) and intestinal (FaSSIF; pH 6.5) media and fed-state gastric (FeSSGF; pH 4.5) and intestinal (FeSSIF; pH 6.0) media, according to the manufacturer's protocol (biorelevant.com, London, UK). Pancreatin extracts (containing lipase, colipase and other nonspecific hydrolytic enzymes) were prepared by stirring 2 g of pancreatin powder in 10 mL of intestinal lipolysis buffer (pH 6.5) for 15 min, followed by centrifugation (2268 rcf, 20 min, 4 °C). The supernatant was collected in a glass vial and kept refrigerated.

In Vitro Drug Solubilization Studies—Lurasidone Solubilization Studies Under Simulated Intestinal Digestion: The aqueous solubilization of lurasidone was quantified during in vitro gastrointestinal lipolysis using a Metrohm 902 Titrando pH-stat titration apparatus equipped with a Dosino 800 dosing apparatus (Herisau, Switzerland). Formulation corresponding to 2 mg lurasidone was added to a temperature-controlled vessel containing 10 mL of either FaSSGF (pH 1.6) or FeSSGF (pH 4.5), maintained at 37 °C. Gastric lipolysis was initiated by the addition of *Candida* lipase (600

tributyrin units lipase activity) and allowed to proceed for 30 min. Following gastric lipolysis, 18 mL of FaSSIF (pH 6.5) or FeSSIF (pH 6.0) media was added to the reaction vessel, where intestinal lipolysis was initiated by the addition of 2 mL pancreatin extract. Aliquots (1 mL) were withdrawn periodically, and lipase was inhibited by the addition of 10 µL of 4-BBA (0.5 M in methanol). Samples were centrifuged (35170 g, 10 min, 37 °C) and the resulting supernatant underwent solvent extraction using acetonitrile via sonication (10 min). This mixture was further centrifuged (21130 g, 10 min, 24 °C) and the supernatant was appropriately diluted for LCMS analysis. Fed: fasted variability was quantified within this study by comparing the area-under-the-curve (AUC) of intestinal lurasidone solubilization profiles between the fed and fasted state for each formulation.

Throughout the intestinal lipolysis phase, fatty acids were automatically titrated with 0.6 M NaOH to maintain the constant predetermined pH. The cumulative volume of NaOH was converted to the molar concentration of fatty acids liberated to determine the rate and extent of lipid digestion. It is important to note that fatty acids produced are protonated at pH 1.6 and therefore NaOH titration is not feasible for fasted-state gastric lipolysis. Subsequently, only intestinal lipolysis data is presented within this study.

In Vivo Studies: Animal studies were reported in accordance with the ARRIVE guidelines for the accurate and reproducible reporting of animal research and complied with the Principles of Laboratory Animal Care (NIH publication #85-23, revised in 1985) and the National Health and Research Council (Australia) Code of Practice for Animal Care in Research and Training (2014). Rats were housed in a temperature-, humidity- and pressure-controlled animal holding facility with a 12 h/12 h light/ dark cycle. Rats were randomized upon arrival at the animal holding facility. Researchers were not blinded to the group allocations at any stage of the experimentation or analysis.

Oral Pharmacokinetic Study: The oral pharmacokinetic animal study was approved by the South Australian Animal Ethics Committee under approval number U05-20 and was performed on six-week-old male rats ($n = 4$) sourced from OzGene (Canning Vale, Australia). The sample size for each group ($n = 4$) was based on Power calculations for anticipated changes in area-under-the-curve, using a power level of ≥0.8 and a significance level of 0.05. A single gender was used for the pharmacokinetics study to minimise gender-based variation commonly observed in oral pharmacokinetics investigations. A lurasidone dose of 20 mg k^{-1} g (suspended in 0.5% w/v carboxymethyl cellulose solution) was administered via oral gavage for each formulation. Rats were singularly housed in the Raturn, equipped with an automatic blood sampling system (BASi Culex NxT, Lafayette, IN, United States) according to the previous study by Meola et al.[16] Rats were allowed ad libitum access to water and were fasted overnight prior to dosing. Blood samples (200 µL) were automatically withdrawn periodically from the jugular vein. Plasma was collected by centrifugation (5000 g, 24 °C, 5 min), diluted with acetonitrile (5:9 ratio) and spiked with internal standard (ziprasidone; 10 µL) for LCMS analysis. Pharmacokinetic analyses were conducted using Phoenix WinNonlin Version 8.3 (Pharsight, a Certara company), via noncompartmental methods (Model 200–202, Extravascular Input) and a linear-trapezoidal approach, as previously reported.[16]

Oral Pharmacomicrobiomic Study: A 21-day, daily dosing study in rats was performed to investigate the impact of each lurasidone formulation on the gut microbiome. The study was approved by the South Australian Animal Ethics Committee under approval number U38-22 and was performed in 8-week-old rats ($n = 8$) sourced from OzGene (Canning Vale, Australia). The sample size for each group ($n = 8$) was based on Power calculations for anticipated changes in Shannon's Index (microbiota alpha diversity), using a power level of ≥0.8 and a significance level of 0.05. An even distribution of male and female rats was allocated per group (four males, four females). Rats were housed in groups of two with ad libitum access to food and water throughout (note: lurasidone formulations were not dosed in the fasted state for the multiple-dosing study). Each lurasidone formulation was dispersed in PBS prior to daily administration between 16:00 and 18:00 via oral gavage over a 3-week period. A reduced lurasidone dose of 7.5 mg k^{-1} g was selected for each formulation for the multiple daily dosing study, where the dosage frequency and length were selected to replicate a chronic dosage regimen. Evening dosing was selected in an attempt to simulate rodents' natural behaviour since they are most active and eat mostly at night. On Day 22 (i.e., the morning after the final dose), rats were anaesthetized with (200 mg k^{-1} g) ilium sodium pentobarbital (60 mg mL^{-1}), prior to cardiac puncture.

Gut Microbiota Analyses: Faecal samples were collected on Days 0 and 21 and sent for DNA extraction, PCR amplification, and 16S rRNA sequencing at the Australian Genomics Research Facility (Brisbane, Australia). DNA was extracted from one faecal pellet per animal per time point to ensure microbiota signatures could be traced back to individual animals and time points. 16S rRNA sequences were processed for the V3-V4 hypervariable regions and raw reads were clustered (97% similarity) to operational taxonomic units (OTUs) on Quantitative Insights into Microbiology Ecology (QIIME 1.8) using the Silva reference database. OTUs were assigned taxonomy using the Qiagen Microbial Insights – Prokaryotic Taxonomy Database (QMI-PTDB) on Qiagen CLC Genomics Workbench version 23.0.4 (Hilden, Germany). The Qiagen genomics module was used to derive alpha diversity at the genus level using Shannon's Index and beta diversity Principal Coordinate Analyses (PCoAs) based on Bray–Curtis dissimilarity metrics. Permutational multivariate ANOVA (PERMANOVA) of beta diversity plots was used to determine the statistical significance of microbiota dissimilarities between groups.

ELISA Assays for Quantifying Pro-Inflammatory Cytokines and Serotonin Levels: Enzyme-linked immunosorbent assays (ELISA; Invitrogen) were performed to quantify the levels of pro-inflammatory cytokines, being interleukin 1 beta (IL-1β), interleukin 6 (IL-6), and tumour necrosis factor-alpha (TNF-α), within the jejunum and serotonin (5-hydroxytryptamine; 5-HT) within the jejunum, faeces, and plasma. The LOQ for IL-1β, IL-6, TNF-α, and 5-HT was 4, 12, 11, and 293 pg mL^{-1}, respectively. Briefly, tissues (≈30 mg) were weighed and homogenized in 500 µL RIPA buffer (ThermoFisher Scientific, Australia), with protease inhibitor cocktail (ThermoFisher Scientific, Australia) added at 1:100 dilution, prior to quantifying protein concentration using a BCA Protein Assay kit (ThermoFisher Scientific, Australia). Normalized protein concentrations (1000 µg mL^{-1}) of tissue/ faecal homogenate were processed according to the manufacturer's instructions with absorbance measured at 450 nm. Cytokine and 5-HT concentrations were calculated according to the standard curve.

Statistical Analysis: All statistical analyses (excluding 16S data) of experimental data were performed using GraphPad Prism Version 8.0 (GraphPad Software Inc., California). Statistically significant differences were determined using an unpaired *t*-test and one-way ANOVA followed by Tukey's post-test for multiple comparisons. Values are reported as the mean ± standard deviation (SD), and the data were considered statistically significant when $p < 0.05$. Statistical significance is represented in figures by $^{*}p < 0.05$, $^{**}p < 0.005$, $^{***}p < 0.0005$ or $^{****}p < 0.0005$.

Ethics Approval: Animal ethics were obtained and approved by the South Australian Animal Ethics Committee.

Acknowledgements

The Hospital Research Foundation (THRF) Group are gratefully acknowledged for their EMCR Fellowship funding and generous support provided to Dr Paul Joyce (2022-CF-EMCR-004-25314). The authors acknowledge the instruments and expertise of Microscopy Australia at Adelaide Microscopy, The University of Adelaide, enabled by NCRIS, university, and state government support. PJ is funded by The Hospital Research Foundation Group.

Open access publishing facilitated by University of South Australia, as part of the Wiley - University of South Australia agreement via the Council of Australian University Librarians.

Conflict of Interest

The authors declare no conflict of interest.

Data Availability Statement

The data that support the findings of this study are available from the corresponding author upon reasonable request.

Keywords

bioavailability, gut-brain axis, lipid formulation, microbiome, oral drug delivery, pharmaceutical food effect, pharmacomicrobiomics

Received: March 4, 2024
Revised: April 7, 2024
Published online:

[1] C. Long-Smith, K. J. O'Riordan, G. Clarke, C. Stanton, T. G. Dinan, J. F. Cryan, *Annu. Rev. Pharmacol. Toxicol.* **2020**, *60*, 477.
[2] R. Mittal, L. H. Debs, A. P. Patel, D. Nguyen, K. Patel, G. O'Connor, M. Grati, J. Mittal, D. Yan, A. A. Eshraghi, *J. Cell. Physiol.* **2017**, *232*, 2359.
[3] Y. Chen, J. Xu, Y. Chen, *Nutrients* **2021**, *13*, 2099.
[4] A. Minichino, T. Preston, J. B. Fanshawe, P. Fusar-Poli, P. McGuire, P. W. Burnet, B. R. Lennox, *Biol. Psychiatry* **2023**, *95*, 611.
[5] S. Cussotto, G. Clarke, T. G. Dinan, J. F. Cryan, *Psychopharmacology* **2019**, *236*, 1411.
[6] L. Qian, X. He, Y. Liu, F. Gao, W. Lu, Y. Fan, Y. Gao, W. Wang, F. Zhu, Y. Wang, *Microbiol. Spectr.* **2023**, *11*, e00058.
[7] Z. Zhu, Y. Gu, C. Zeng, M. Yang, H. Yu, H. Chen, B. Zhang, H. Cai, *Front. Pharmacol.* **2022**, *13*, 897926.
[8] S. Bahr, B. Tyler, N. Wooldridge, B. Butcher, T. Burns, L. Teesch, C. Oltman, M. Azcarate-Peril, J. Kirby, C. Calarge, *Transl. Psych.* **2015**, *5*, e652.
[9] S. M. Bahr, B. J. Weidemann, A. N. Castro, J. W. Walsh, O. Deleon, C. M. Burnett, N. A. Pearson, D. J. Murry, J. L. Grobe, J. R. Kirby, *EBioMed.* **2015**, *2*, 1725.
[10] S. Kamath, A. Hunter, K. Collins, A. Wignall, P. Joyce, *bioRxiv* **2024**, 582623.
[11] S. Preskorn, L. Ereshefsky, Y. Y. Chiu, N. Poola, A. Loebel, *Hum. Psychopharmacol.: Clin. Exp.* **2013**, *28*, 495.
[12] L. Citrome, *Adv. Ther.* **2012**, *29*, 815.
[13] R. R. Jaeschke, M. Sowa-Kućma, P. Pańczyszyn-Trzewik, P. Misztak, K. Styczeń, W. Datka, *Pharmacol. Rep.* **2016**, *68*, 748.
[14] W. M. Greenberg, L. Citrome, *Clin. Pharmacokinet.* **2017**, *56*, 493.
[15] F. Jangipuria, V. Londhe, *Int. J. Pharm. Sci.* **2015**, *7*, 283.
[16] T. R. Meola, P. Joyce, A. Wignall, K. E. Bremmell, C. A. Prestidge, *Int. J. Pharm.* **2021**, *608*, 121098.
[17] M. H. Patel, V. P. Mundada, K. K. Sawant, *Drug Dev. Ind. Pharm.* **2019**, *45*, 1242.
[18] Y. Miao, J. Sun, G. Chen, R. Lili, P. Ouyang, *Drug Dev. Ind. Pharm.* **2016**, *42*, 1234.
[19] S. Subramaniam, A. Elz, A. Wignall, S. Kamath, A. Ariaee, A. Hunter, T. Newblack, H. R. Wardill, C. A. Prestidge, P. Joyce, *Int. J. Pharm.* **2023**, *648*, 123614.
[20] S. Subramaniam, S. Kamath, A. Ariaee, C. Prestidge, P. Joyce, *Expert Opin. Drug Deliv.* **2023**, *20*, 1297.
[21] S. Naimi, E. Viennois, A. T. Gewirtz, B. Chassaing, *Microbiome* **2021**, *9*, 66.
[22] S. Kamath, A. M. Stringer, C. A. Prestidge, P. Joyce, *Expert Opin. Drug Deliv.* **2023**, *20*, 1315.
[23] A. C.-C. Kao, S. Spitzer, D. C. Anthony, B. Lennox, P. W. Burnet, *Transl. Psychiat.* **2018**, *8*, 66.
[24] J. Huang, D. Kang, F. Zhang, Y. Yang, C. Liu, J. Xiao, Y. Long, B. Lang, X. Peng, W. Wang, *Schizophr. Bull.* **2022**, *48*, 850.
[25] S. A. Flowers, N. T. Baxter, K. M. Ward, A. Z. Kraal, M. G. McInnis, T. M. Schmidt, V. L. Ellingrod, *Pharmacotherapy* **2019**, *39*, 161.
[26] C. Barrera-Bugueño, O. Realini, J. Escobar-Luna, R. Sotomayor-Zárate, M. Gotteland, M. Julio-Pieper, J. A. Bravo, *Neuroscience* **2017**, *359*, 18.
[27] C. Amadieu, V. Coste, A. M. Neyrinck, V. Thijssen, Q. Leyrolle, L. B. Bindels, H. Piessevaux, P. Stärkel, P. de Timary, N. M. Delzenne, *Gut Microbes* **2022**, *14*, 2007042.
[28] A. P. Smith, D. Sutherland, P. Hewlett, *Nutrients* **2015**, *7*, 8887.
[29] P. P. Jackson, A. Wijeyesekera, C. M. Williams, S. Theis, J. van Harsselaar, R. A. Rastall, *Am. J. Clin. Nutr.* **2023**, *118*, 938.
[30] L. Guo, P. Xiao, X. Zhang, Y. Yang, M. Yang, T. Wang, H. Lu, H. Tian, H. Wang, J. Liu, *Food Funct.* **2021**, *12*, 1156.
[31] D. L. Kelly, M. A. Kane, C. M. Fraser, M. A. Sayer, S. Grant-Beurmann, T. Liu, J. M. Gold, F. M. Notarangelo, G. R. Vyas, C. M. Richardson, S. M. August, B. Kotnana, J. Miller, F. Liu, R. W. Buchanan, *J. Clin. Psychopharmacol.* **2021**, *41*, 200.
[32] P. Joyce, C. A. Prestidge, *Eur. J. Pharm. Sci.* **2018**, *118*, 40.
[33] R. Almasri, P. Joyce, H. B. Schultz, N. Thomas, K. E. Bremmell, C. A. Prestidge, *Pharmaceutics* **2020**, *12*, 687.
[34] S. Maghrebi, N. Thomas, C. A. Prestidge, P. Joyce, *Drug Deliv. Transl. Res.* **2023**, *13*, 1716.
[35] D. B. Warren, H. Benameur, C. J. Porter, C. W. Pouton, *J. Drug Targeting* **2010**, *18*, 704.
[36] E. J. Suys, D. K. Chalmers, C. W. Pouton, C. J. Porter, *Mol. Pharmaceutics* **2018**, *15*, 2355.
[37] J. Khan, T. Rades, B. Boyd, *Pharm. Res.* **2016**, *33*, 548.
[38] A.-R. Ilie, B. T. Griffin, M. Vertzoni, M. Kuentz, R. Kolakovic, A. Prudic-Paus, A. Malash, H. Bohets, J. Herman, R. Holm, *Eur. J. Pharm. Sci.* **2021**, *159*, 105691.
[39] H. Y. Meltzer, B. W. Massey, *Curr. Opin. Pharmacol.* **2011**, *11*, 59.
[40] N. Terry, K. G. Margolis, *Handb. Exp. Pharmacol.* **2017**, *239*, 319.
[41] B. A. Everett, P. Tran, A. Prindle, *Curr. Opin. Biotechnol.* **2022**, *78*, 102826.
[42] T. B. Legan, B. Lavoie, G. M. Mawe, *Neurogastroenterol. Motil.* **2022**, *34*, e14346.